crystals

MDPI

Article

Fine Fabrication and Optical Waveguide Characteristics of Hexagonal tris(8-hydroxyquinoline)aluminum(III) (Alq_3) Crystal

Jungwoon Park †, Seokho Kim †, Jinho Choi, Sung Ho Yoo, Seongjae Oh, Do Hyoung Kim and Dong Hyuk Park *

Department of Chemical Engineering, Inha University, Incheon 22212, Korea; jungwoon@inha.edu (J.P.); seokho@inha.edu (S.K.); jinho@inha.edu (J.C.); yoosh@inha.edu (S.H.Y.); 12140769@inha.edu (S.O.); gg1236@inha.edu (D.H.K.)

* Correspondence: donghyuk@inha.ac.kr; Tel.: +82-32-860-7496

† These authors contributed equally.

Received: 29 February 2020; Accepted: 27 March 2020; Published: 30 March 2020

Abstract: Herein, we reported on the precise growth and optical waveguide characteristics of hexagonal tris(8-hydroxyquinoline)aluminum(III) (Alq_3) micro-crystals (MCs). The hexagonal Alq_3 MCs were prepared using surfactant-assisted assembly growth with the help of cetyltrimethylammoniumbromide (CTAB), in which the crystallization occurred as a result of molecular assembly and packing. Also, we adjusted the molar ratio of Alq_3 and CTAB for the control degree of crystallization. The formation and structure of Alq_3 MCs were investigated using field-emission scanning electron microscopy and X-ray diffraction pattern experiments, respectively. The solid-state laser confocal microscope-photoluminescence spectra and charge-coupled device images for the Alq_3 MCs were measured to study the luminescence efficiency and colors, respectively. The optical waveguide performance of the hexagonal Alq_3 MCs was measured for each side direction. According to our results, crystalline Alq_3 micro-crystals are promising materials for application to the development of optical communication devices.

Keywords: organometal; Alq_3; crystallinity; surfactant; photoluminescence; waveguide; confocal microscope

1. Introduction

The development of optoelectronic devices based on smart functional organic materials has recently drawn much attention because of their promising practical applications [1,2]. Among various configurations, highly crystalline organic materials are of particular interest as they can serve as ideal platforms for advanced optoelectronic applications with good stability and charge transfer properties [3–5]. Organic crystal structures offer unique advantages, such as relatively high electrical performance and good processability, making them complementary to inorganic materials, which have been demonstrated in light-emitting diodes, photovoltaic cells, field-effect transistors, optical waveguides, and lasers [6–10]. In particular, crystalline structures of organic molecules with remarkably improved optoelectronic characteristics are achievable, enabling propagation of emission by active optical waveguiding in a crystal [11–13].

To achieve high luminescence characteristics, densely-stacked molecules, and large grain sizes, single crystallinity is usually required. Therefore, our materials can exhibit high-efficiency emission with a self-assembled structure that can produce single-crystalline materials without any local impurities and extended defects [14]. In addition, the improvement of crystallinity is always a problem in organic

crystal structures, in which high charge transport mobility and remarkable optical behaviors are expected in highly ordered crystal structures [15–18].

Herein, we investigated the precise control of growth conditions and optical waveguide characteristics based on hexagonal tris(8-hydroxyquinoline)aluminum(III) (Alq_3) micro-crystals (MCs). Unlike previous reports, we introduced the ideal experimental construction of crystal structures with high crystallinity using simple surfactant-assisted assembly growth in a de-ionized (DI) water solution [19]. It is important to optimize the growth conditions, such as the moral ratio between organic molecules and surfactants, because the role of surfactant is very important in crystal growth, and crystallinity is closely related to optical properties [20]. Optical properties are determined by the behavior of the exciton. In general, the exciton of well-formed crystal has a high degree of freedom and has excellent optical properties [21,22]. The assembly of molecules to hexagonal crystals with well-defined morphologies requires driving forces from the molecules themselves, including molecular stacking and Van der Waals forces [23–26]. A process using the cetyltrimethylammoniumbromide (CTAB) surfactant induced the self-assembly of Alq_3 molecules by these driven forces.

The results were confirmed by scanning electron microscopy (SEM) and X-ray diffraction (XRD) experiments. The solid-state laser confocal microscope (LCM)-photoluminescence (PL) spectra and color charge-couple device (CCD) images for the Alq_3 MCs were acquired to study the luminescence efficiency and colors, respectively. The optical waveguide performance of the hexagonal Alq_3 MCs was measured for each side direction. The results demonstrated that crystalline organic materials could potentially be applied to the development of optical communication devices with high optical waveguide emission performance.

2. Materials and Methods

2.1. Materials and Preparation

Chemical reagent: the tris(8-hydroxyquinoline)aluminum(III) (Alq_3, $C_{27}H_{18}AlN_3O_3$, purity 99.995%) and cetyltrimethylammoniumbromide (CTAB, $CH_3(CH_2)_{15}N(Br)(CH_3)_3$, purity 99%) used in the experiment were purchased from Sigma Aldrich (Darmstadt, Germany). Alq_3 was dissolved in chloroform to achieve a concentration of 10 mM. Alq_3 was blended with chloroform using a hot-plate magnetic stirrer to ensure that it dissolves perfectly, and CTAB was prepared in DI water to reach a concentration of 10 mM.

The CTAB solution was placed into a 20 mL vial and stirred vigorously on a magnetic hot-plate. Alq_3 solution was added and strongly sprayed on the CTAB solution using a micropipette. The cap of the vial was then closed, and stirring was maintained at high rpm for 5 min. The mixing solution was kept on a 70 °C hot-plate for 8 h. Other solutions with the same ingredients and various amounts of CTAB were prepared (Figure 1).

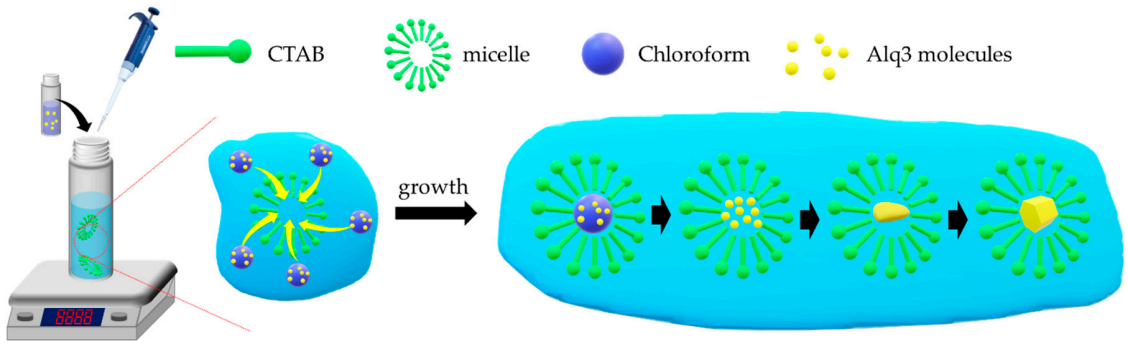

Figure 1. Schematic illustration of surfactant micelle-induced tris(8-hydroxyquinoline)aluminum(III) (Alq_3) micro-crystal (MC) growth. CTAB, cetyltrimethylammoniumbromide.

2.2. Measurement

The shape and size of the Alq_3 MCs were analyzed using field-emission SEM (Hitachi, SU-8010, Tokyo, Japan) with an acceleration voltage of 15 kV. The XRD (X'Pert Powder Diffractometer, Malvern Panalytical Ltd., Malvern, United Kingdom) spectra were captured at a voltage of 40 kV and a current of 40 mA with Cu-Kα radiation (λ = 1.540 Å). The scanning rate was 0.02°/s, and the 2θ range was captured from 5° to 60°. PL CCD images of the Alq_3 were acquired using an AVT Marlin F-033C (λ_{ex} = 435 nm) (Allied Vision, Exton, PA, USA). To compare the brightness (i.e., PL intensity) of the CCD images of Alq_3 MCs, the exposure time with the energy source was fixed at 0.1 s. LCM PL spectra were acquired using a homemade LCM instrument (Axiovert 200, Zeiss GmbH, Oberkochen, Germany). The 405 nm unpolarized diode laser line was used for the LCM PL excitation. The Alq_3 MCs were located on a cover glass, which was placed on the XY piezo stage of the instrument. An oil-immersion objective lens (N.A. of 1.4) was used to focus the unpolarized laser light on the crystal surface. The beam size of the focused laser on the sample was calculated to be approximately 200 nm. The scattered light from Alq_3 MCs was collected through the same objective lens. The excitation laser (λ = 405 nm) light was filtered out using a long-pass edge-filter (Semrock, Rochester, New York, USA). The red-shifted PL signal caused by the Stokes shift was collected with a multimode fiber (core size = 50 μm) that acted as a pinhole for the confocal microscope. The opposite end of the multimode fiber was connected to a photomultiplier tube for the PL image or the input slit of a 0.3 m long monochromator equipped with a cooled CCD for PL spectra measurement. Therefore, solid-state PL spectra were analyzed at the nanometer scale. The laser power of the incident laser to reach the sample and the acquisition time for each LCM PL spectrum were fixed at 50 μW and 0.1 s, respectively, for all confocal PL experiments.

3. Results and Discussion

We demonstrated a self-assembled growth of Alq_3 MCs (Figure 1). This interesting material was characterized by a strong self-assembling capability that led to the formation of a crystal wire, exhibiting a dramatic increase in green emission upon the formation of MCs. With a surfactant, micelles were formed in the solution, and growth began inside the micelles. In detail, hydrophilic DI water was a poor solvent for Alq_3, so they tended to aggregate itself. At the same time, CTAB formed micelles that were hydrophobic on the inside and hydrophilic on the outside in DI water. The Alq_3 molecule entered the CTAB micelle to lower surface energy and was aggregated and nucleated. Therefore, the result varied greatly depending on the ratio of surfactant to Alq_3. Figure 2 shows SEM images of structures formed by adjusting the molar ratio of Alq_3 molecules to CTAB as a surfactant. If the critical micelle concentration (CMC) was not reached because of the lack of surfactant, the micelles were not formed in the solution, and the Alq_3 molecules aggregated in random forms. Increasing the amount of surfactant added to the growth reaction produced Alq_3 MCs with a straight shape and ordered surface. Figure 2a shows the growth of only Alq_3 molecules without added surfactant, and the molar fractions of Alq_3:CTAB in Figure 2b–e were 1:0.1, 1:0.3, 1:0.6, and 1:1, respectively. At the molar fractions shown in Figure 2c and higher, the CMC of CTAB was reached, and the form of MCs appeared. The length and diameter of crystals in Figure 2c,d were 10 μm and 1 μm, respectively. Also, crystals from Figure 2e had 12~15 μm and 2 μm, respectively. As the amount of surfactant increased, the diameter was thicker than the lengthwise growth. Some crystals were grown well, even with a lack of CTAB, but they tended to be less uniform in shape and size. With an excess amount of CTAB, many micelles were produced, and nucleation occurred, so crystals did not grow and remained as small particles.

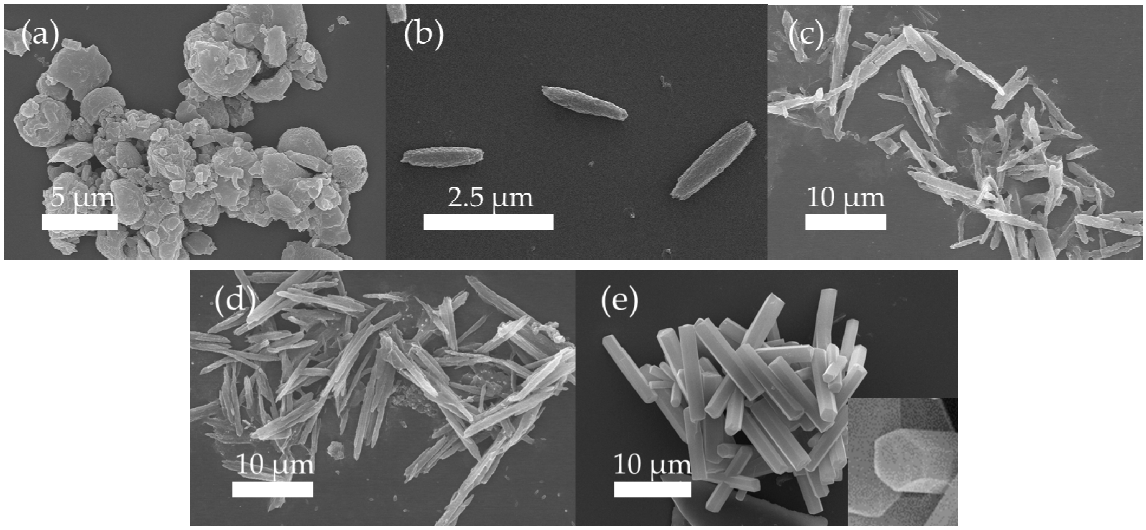

Figure 2. Morphological analyses of Alq_3 MCs. (**a–e**) SEM images of Alq_3 MCs after assembly with various amounts of surfactant. The molar fractions of Alq_3:CTAB in (**a–e**) were 1:0, 1:0.1, 1:0.3, 1:0.6, and 1:1, respectively. (Inset of (**e**): magnification cross-section image of Alq_3 micro-rod).

XRD measurements were performed to analyze the effect of various amounts of surfactant on the crystallinity during the crystal growth process. The XRD spectra, shown in Figure 3, corresponded to the Alq_3 MCs of Figure 2a,e, assigned planes (001), (010), (011), and (021) with 2-theta values of 6.3°, 7.0°, 11.4°, and 17.9°, respectively [27]. The as-grown Alq_3 MCs showed a typical α-phase and showed increasing crystallinity with increasing amounts of CTAB (from Figure 2b (molar ratio 1:0.1) to Figure 2e, (molar ratio 1:1.0)). Crystals of α-Alq_3 were triclinic, space group P−1, a = 13.58 Å, b = 12.44 Å, c = 7.75 Å, respectively. Also, we could reasonably infer that α = 69.90°, β = 89.47°, γ = 82.52° according to the XRD spectra and Rajeswaran's results [25,28]. Therefore, CTAB could control both the crystallinity as well as morphology, such as the shape and size of Alq_3 MCs (CCDC, Refcode QATMON01) [29].

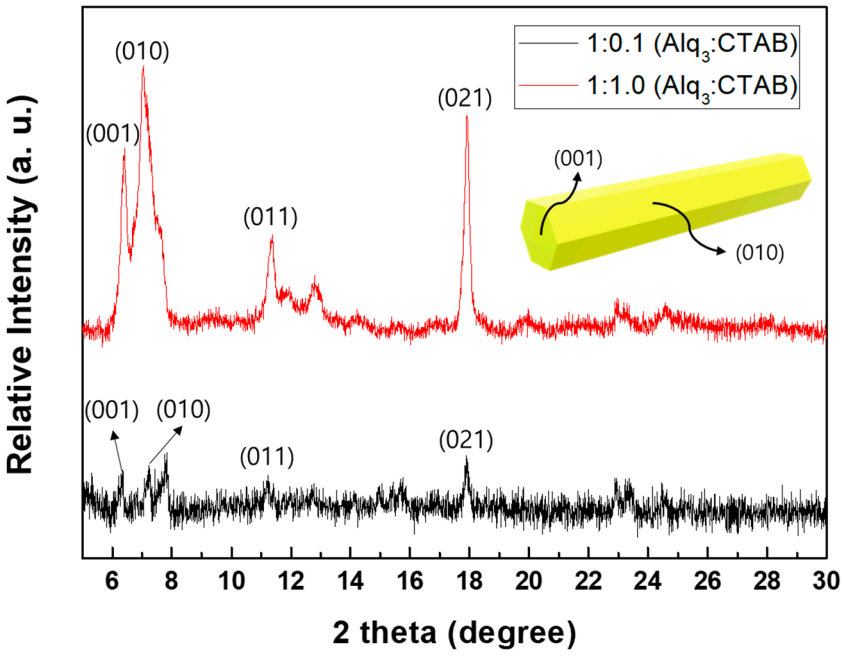

Figure 3. XRD spectra of crystals whose molar ratio with Alq_3 and CTAB were 1:0.1 (top, red line) and 1:1.0 (bottom, black line). (inset: schematic illustration of crystal with lattice plane).

Based on its high quantum yield, Alq_3 has been used in various optoelectronic fields as a green light-emitting layer from the early stage of organic light emitting diodes (OLED) development. Alq_3 showed strong green fluorescence when irradiated with 405 nm energy, and the main peak was measured at 520 nm, as shown in Figure 4. In many previous studies, it was difficult to quantitatively compare the PL characteristics, such as the intensity or full width at half maximum (FWHM), of Alq_3 crystals by using bulk CCDs or by measuring solid PL in solution or large areas [30–32].

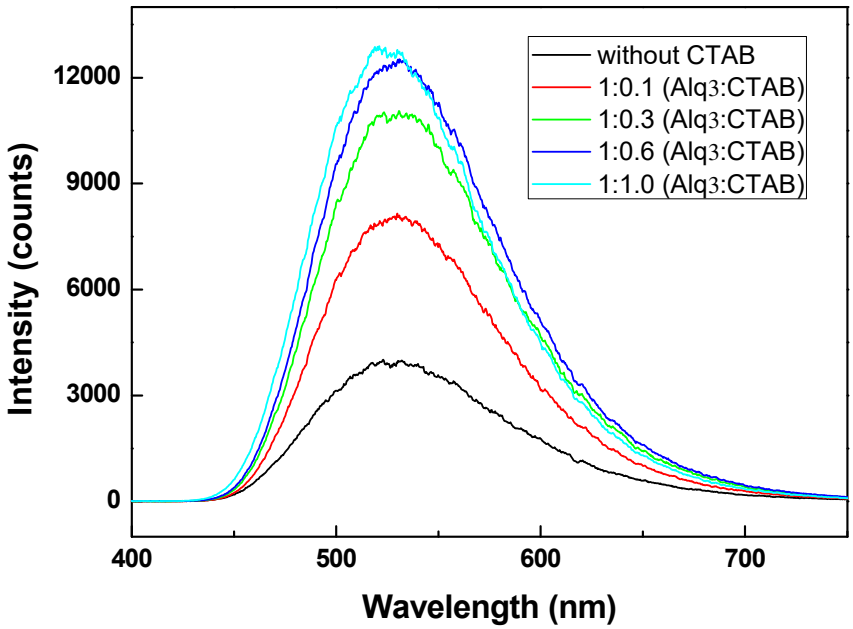

Figure 4. PL (photoluminescence) spectra of Alq_3 MCs depending on the molar ratio of Alq_3 to CTAB.

In this study, a quantitative comparison was performed by measuring solid PL from a single Alq_3 crystal using a laser with a spot size of approximately 200 nm. This figure showed that the PL signal was measured even in amorphous random structures mass-created without CTAB. To compare the PL intensity as quantitatively as possible, the same energy was irradiated and measured for a single unit of Alq_3 MCs. The better crystallization and alignment of the molecules could increase the intensity of the PL because the disturbance is reduced during emission when excited electrons move to the ground state. In addition, a smoother crystal surface led to less scattering of incident energy and emitted fluorescence, which increased the intensity of PL because more light could be gathered to pass into the detector. However, some PL intensity was measured even in the absence of CTAB because of the lack of a uniform shape and presence of relatively many Alq_3 molecules per unit area.

The highly crystalline structures of Alq_3 MCs could conduct photon propagation along the direction of crystal packing. Therefore, we could obtain optically active PL waveguide performance. A schematic illustration of an optical waveguide experiment is shown in Figure 5a. The excitation position was presented as a bright green luminescence spot in the color CCD images in the inset of Figure 5b, and the position could be moved along the axial direction of Alq_3 MCs. It showed very bright luminescence spots at both tips and relatively weaker emission from the bodies of the wires, which are typical characteristics of an optical active waveguide caused by self-absorption. From the out-coupled luminescence CCD images and PL spectra results, the emission intensity was relatively weak at the endpoint, and the main peaks of the guided PL spectra gradually decreased with increasing propagation length, which could be attributed to the re-absorption energy loss process of the guided light during propagation caused by the interaction, such as total reflection, due to difference in dielectric constant between crystal surface and surrounding atmosphere or substrate, as shown in Figure 5b.

The original PL main peak for the Alq_3 material at 520 nm was filtered through reabsorption during propagation, and the output PL peaks were observed at 525 nm, as shown in Figure 5b.

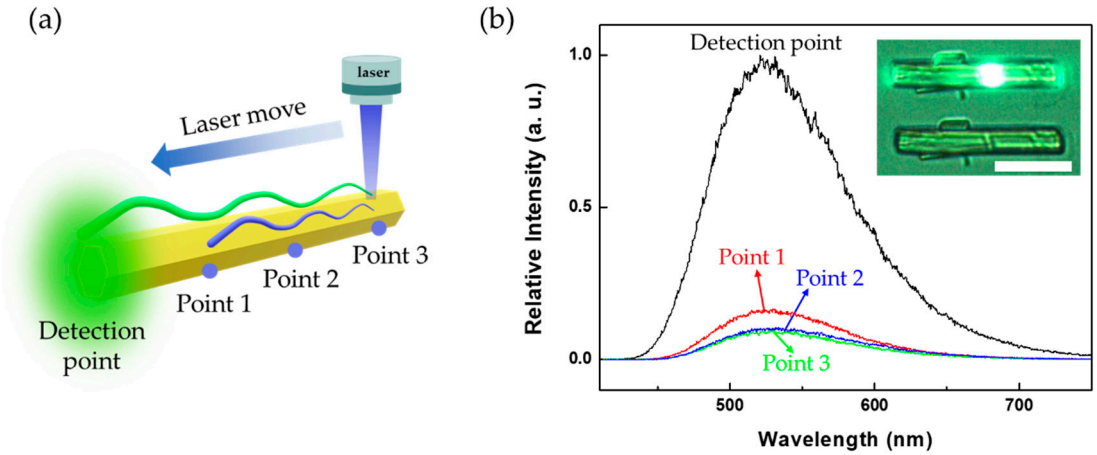

Figure 5. (**a**) Schematic illustration of an optical waveguide with a movable laser and fixed detector system. (**b**) PL waveguide spectra of single Alq_3 MCs (λex: 405 nm, scale bar: 5 μm).

From the calculation of the intensity of main PL peaks, the average decay constant for the Alq_3 MCs was estimated to be 0.381 dB/μm. Considering that the propagated optical signal was measured, we suggested that they are a good candidate for potential materials for application in the development of optical communication devices [33,34].

4. Conclusions

We investigated the precise control of crystallinity with various amounts of CTAB and the optical waveguide performance of hexagonal Alq_3 MCs. Unlike previous reports, we proposed an ideal growth condition for the crystal structure with high crystallinity by a simple surfactant-assisted self-assembly method in DI water. Hexagonal crystals with well-defined morphologies required driving forces from the molecules themselves, including molecular stacking and Van der Waals forces. The CTAB surfactant could cause micelles in DI water to induce the self-assembly of Alq_3 molecules by these driven forces. We confirmed the dimensions and morphological properties using SEM and XRD experiments. Furthermore, we measured the solid-state LCM-PL spectra and color CCD images of the Alq_3 MCs to determine the PL efficiency and colors, respectively. The Alq_3 MCs demonstrated optical waveguide performance for each side direction of the hexagonal-shape. Our results demonstrated that crystalline organic materials are promising materials for application to the development of optical communication devices with high optical waveguide emission performance.

Author Contributions: Conceptualization, S.K. and D.H.P.; Data curation, S.H.Y., S.O., and D.H.K.; Formal analysis, J.C. and D.H.P.; Funding acquisition, D.H.P.; Investigation, J.P.; Project administration, D.H.P.; Supervision, D.H.P.; Writing—original draft, J.P. and S.K.; Writing—review and editing, S.K. and D.H.P. All authors have read and agreed to the published version of the manuscript.

Funding: This work was supported by INHA UNIVERSITY Research Grant 60586.

Conflicts of Interest: The authors declare no conflict of interest.

References

1. Zhao, Y.S.; Fu, H.; Peng, A.; Ma, Y.; Xiao, D.; Yao, J. Low-dimensional Nanomaterials Based on Small Organic Molecules: Preparation and Optoelectronic Properties. *Adv. Mater.* **2008**, *20*, 2859–2876. [CrossRef]
2. Zhao, Y.S.; Fu, H.B.; Hu, F.Q.; Peng, A.D.; Yang, W.S.; Yao, J.N. Tunable Emission from Binary Organic One-dimensional Nanomaterials: An Alternative Approach to White-light Emission. *Adv. Mater.* **2008**, *20*, 79–83. [CrossRef]

3. Park, D.H.; Kim, M.S.; Joo, J. Hybrid Nanostructures using Π-Conjugated Polymers and Nanoscale Metals: Synthesis, Characteristics, and Optoelectronic Applications. *Chem. Soc. Rev.* **2010**, *39*, 2439–2452. [CrossRef]
4. Heeger, A.J. Semiconducting Polymers: The Third Generation. *Chem. Soc. Rev.* **2010**, *39*, 2354–2371. [CrossRef]
5. Jo, S.G.; Park, D.H.; Kim, B.; Seo, S.; Lee, S.J.; Kim, J.; Kim, J.; Joo, J. Dual-Mode Waveguiding of Raman and Luminescence Signals in a Crystalline Organic Microplate. *J. Mater. Chem. C* **2014**, *2*, 6077–6083. [CrossRef]
6. Yan, R.; Gargas, D.; Yang, P. Nanowire Photonics. *Nat. Photon.* **2009**, *3*, 569–576. [CrossRef]
7. Cui, Q.H.; Zhao, Y.S.; Yao, J. Photonic Applications of One-Dimensional Organic Single-Crystalline Nanostructures: Optical Waveguides and Optically Pumped Lasers. *J. Mater. Chem.* **2012**, *22*, 4136–4140. [CrossRef]
8. Zhang, C.; Zhao, Y.S.; Yao, J. Optical Waveguides at Micro/Nanoscale Based on Functional Small Organic Molecules. *Phys. Chem. Phys.* **2011**, *13*, 9060–9073. [CrossRef] [PubMed]
9. Anthony, J.E. Functionalized Acenes and Heteroacenes for Organic Electronics. *Chem. Rev.* **2006**, *106*, 5028–5048. [CrossRef] [PubMed]
10. Briseno, A.L.; Holcombe, T.W.; Boukai, A.I.; Garnett, E.C.; Shelton, S.W.; Fréchet, J.J.; Yang, P. Oligo-and Polythiophene/ZnO Hybrid Nanowire Solar Cells. *Nano Lett.* **2010**, *10*, 334–340. [CrossRef] [PubMed]
11. Cho, E.H.; Kim, B.; Jun, S.; Lee, J.; Park, D.H.; Lee, K.; Kim, J.; Kim, J.; Joo, J. Remote Biosensing with Polychromatic Optical Waveguide using Blue Light-Emitting Organic Nanowires Hybridized with Quantum Dots. *Adv. Funct. Mater.* **2014**, *24*, 3684–3691. [CrossRef]
12. Jo, S.G.; Kim, B.G.; Kim, J.; Kim, J.; Joo, J. Waveguiding Characteristics of Surface Enhanced Raman Scattering Signals Along Crystalline Organic Semiconducting Microrod. *Opt. Express* **2017**, *25*, 6215–6226. [CrossRef]
13. Lee, J.W.; Kim, K.; Jung, J.S.; Jo, S.G.; Kim, H.; Lee, H.S.; Kim, J.; Joo, J. Luminescence, Charge Mobility, and Optical Waveguiding of Two-Dimensional Organic Rubrene Nanosheets: Comparison with One-Dimensional Nanorods. *Org. Electron.* **2012**, *13*, 2047–2055. [CrossRef]
14. Briseno, A.L.; Mannsfeld, S.C.; Lu, X.; Xiong, Y.; Jenekhe, S.A.; Bao, Z.; Xia, Y. Fabrication of Field-Effect Transistors from Hexathiapentacene Single-Crystal Nanowires. *Nano Lett.* **2007**, *7*, 668–675. [CrossRef] [PubMed]
15. Huang, L.; Liao, Q.; Shi, Q.; Fu, H.; Ma, J.; Yao, J. Rubrene Micro-Crystals from Solution Routes: Their Crystallography, Morphology and Optical Properties. *J. Mater. Chem.* **2010**, *20*, 159–166. [CrossRef]
16. Garreau, A.; Duvail, J. Recent Advances in Optically Active Polymer-Based Nanowires and Nanotubes. *Adv. Opt. Mater.* **2014**, *2*, 1122–1140. [CrossRef]
17. Lee, T.; Lin, M.S. Sublimation Point Depression of Tris (8-Hydroxyquinoline) Aluminum (III)(Alq_3) by Crystal Engineering. *Cryst. Growth Des.* **2007**, *7*, 1803–1810. [CrossRef]
18. Xie, W.; Fan, J.; Song, H.; Jiang, F.; Yuan, H.; Wei, Z.; Ji, Z.; Pang, Z.; Han, S. Controllable Synthesis of Rice-Shape Alq_3 Nanoparticles with Single Crystal Structure. *Phys. E Low Dimens. Syst. Nanostruct.* **2016**, *84*, 519–523. [CrossRef]
19. Kim, S.; Kim, D.H.; Choi, J.; Lee, H.; Kim, S.; Park, J.W.; Park, D.H. Growth and Brilliant Photo-Emission of Crystalline Hexagonal Column of Alq_3 Microwires. *Materials* **2018**, *11*, 472. [CrossRef]
20. Fukushima, T.; Kaji, H. Green-and Blue-Emitting Tris (8-Hydroxyquinoline) Aluminum (III)(Alq_3) Crystalline Polymorphs: Preparation and Application to Organic Light-Emitting Diodes. *Org. Electron.* **2012**, *13*, 2985–2990. [CrossRef]
21. Tamura, H.; Hamada, I.; Shang, H.; Oniwa, K.; Akhtaruzzaman, M.; Jin, T.; Asao, N.; Yamamoto, Y.; Kanagasekaran, T.; Shimotani, H. Theoretical Analysis on the Optoelectronic Properties of Single Crystals of Thiophene-Furan-Phenylene Co-Oligomers: Efficient Photoluminescence due to Molecular Bending. *J. Phys. Chem. C* **2013**, *117*, 8072–8078. [CrossRef]
22. Devi, S.R.; Kalaiyarasi, S.; Zahid, I.M.; Kumar, R.M. Studies on the Growth Aspects, Structural, Thermal, Dielectric and Third Order Nonlinear Optical Properties of Solution Grown 4-Methylpyridinium P-Nitrophenolate Single Crystal. *J. Cryst. Growth* **2016**, *454*, 139–146. [CrossRef]
23. Bi, H.; Zhang, H.; Zhang, Y.; Gao, H.; Su, Z.; Wang, Y. Fac-Alq_3 and Mer-Alq_3 Nano/Microcrystals with Different Emission and Charge-Transporting Properties. *Adv. Mater.* **2010**, *22*, 1631–1634. [CrossRef] [PubMed]
24. Cölle, M.; Brütting, W. Thermal, Structural and Photophysical Properties of the Organic Semiconductor Alq_3. *Phys. Status Solidi A* **2004**, *201*, 1095–1115. [CrossRef]

25. Rajeswaran, M.; Blanton, T.N. Single-Crystal Structure Determination of a New Polymorph (E-Alq_3) of the Electroluminescence OLED (Organic Light-Emitting Diode) Material, Tris (8-Hydroxyquinoline) Aluminum (Alq_3). *J. Chem. Cryst.* **2005**, *35*, 71–76. [CrossRef]
26. Cölle, M.; Dinnebier, R.E.; Brütting, W. The Structure of the Blue Luminescent Δ-Phase of Tris (8-Hydroxyquinoline) Aluminium (Iii)(Alq_3). *Chem. Commun.* **2002**, 2908–2909. [CrossRef]
27. Cui, C.; Park, D.H.; Kim, J.; Joo, J.; Ahn, D.J. Oligonucleotide Assisted Light-Emitting Alq_3 Microrods: Energy Transfer Effect with Fluorescent Dyes. *Chem. Commun.* **2013**, *49*, 5360–5362. [CrossRef]
28. Brinkmann, M.; Gadret, G.; Muccini, M.; Taliani, C.; Masciocchi, N.; Sironi, A. Correlation between Molecular Packing and Optical Properties in Different Crystalline Polymorphs and Amorphous Thin Films of Mer-Tris (8-Hydroxyquinoline) Aluminum (III). *J. Am. Chem. Soc.* **2000**, *122*, 5147–5157. [CrossRef]
29. Hu, J.; Ji, H.; Cao, A.; Huang, Z.; Zhang, Y.; Wan, L.; Xia, A.; Yu, D.; Meng, X.; Lee, S. Facile Solution Synthesis of Hexagonal Alq_3 Nanorods and their Field Emission Properties. *Chem. Commun.* **2007**, 3083–3085. [CrossRef]
30. Xu, G.; Tang, Y.; Tsang, C.; Zapien, J.; Lee, C.; Wong, N. Facile Solution Synthesis without Surfactant Assistant for Ultra Long Alq_3 Sub-Microwires and their Enhanced Field Emission and Waveguide Properties. *J. Mater. Chem.* **2010**, *20*, 3006–3010. [CrossRef]
31. Goswami, M.; Nayak, P.K.; Periasamy, N.; Madhu, P.K. Characterisation of Different Polymorphs of Tris (8-Hydroxyquinolinato) Aluminium (III) using Solid-State NMR and DFT Calculations. *Chem. Cent. J.* **2009**, *3*, 1–11. [CrossRef] [PubMed]
32. Bi, H.; Chen, D.; Li, D.; Yuan, Y.; Xia, D.; Zhang, Z.; Zhang, H.; Wang, Y. A Green Emissive Amorphous Fac-Alq_3 Solid Generated by Grinding Crystalline Blue Fac-Alq_3 Powder. *Chem. Commun.* **2011**, *47*, 4135–4137. [CrossRef] [PubMed]
33. Park, H.J.; Kim, M.S.; Kim, J.; Joo, J. Fine Control of Photoluminescence and Optical Waveguiding Characteristics of Organic Rubrene Nanorods using Focused Electron-Beam Irradiation. *J. Phys. Chem. C* **2014**, *118*, 30179–30186. [CrossRef]
34. Cho, E.; Choi, J.; Jo, S.; Park, D.; Hong, Y.K.; Kim, D.; Lee, T.S. A Single-Benzene-Based Fluorophore: Optical Waveguiding in the Crystal Form. *ChemPlusChem* **2019**, *84*, 1130–1134. [CrossRef] [PubMed]